Electronic Supporting information

Luminescent Pt(II) Complexes Featuring Imidazolylidene-Pyridylidene and Dianionic Bipyrazolate: from Fundamentals to OLED Fabrications

Chung-Hao Tseng,[a] Mark A. Fox,[b,*] Jia-Ling Liao,[a] Chia-Hao Ku,[c] Zong-Ting Sie,[c] Chih-Hao Chang,[c,*] Jin-Yun Wang,[d] Zhong-Ning Chen,[d] Gene-Hsiang Lee[e] and Yun Chi[a,*]

[a] Department of Chemistry, National Tsing Hua University, Hsinchu 30013, Taiwan; *E-mail: ychi@mx.nthu.edu.tw

[b] Department of Chemistry, Durham University, South Road, Durham, DH1 3LE, UK; *E-mail: m.a.fox@durham.ac.uk

[c] Department of Photonics Engineering, Yuan Ze University, Chungli 32003, Taiwan; *E-mail: chc@saturn.yzu.edu.tw

[d] Fujian Institute of Research on the Structure of Matter, CAS, State Key Laboratory of Structural Chemistry, China

[e] Instrumentation Center, National Taiwan University, Taipei 10617, Taiwan

Synthesis of $Me_2impy(I)_2$. Imidazole (1.72 g, 25.4 mmol), 3-bromopyridine (1.24 mL, 12.6 mmol), $CuSO_4$ (81 mg, 0.51 mmol), and K_2CO_3 (2.27 g, 16.1 mmol) were heated in a Schlenk flask at 150 °C for 12 h under N_2. After cooled to RT, the resulting brown solid was dissolved in 60 mL of deionized water and extracted with ethyl acetate to obtain a crude 3-(1-imidazolyl)pyridine. Without further purification, this mixture was treated with methyl iodide (2.33 mL, 38.2 mmol) in refluxing CH_3CN (15 mL) for 16 h. The corresponding 1-methyl-3-(1-methyl-imidazolium-3-yl)-pyridinium diiodide ($Me_2impy(I)_2$) was precipitated out as a pale yellow solid. It was then isolated by filtration, washed with minimum amount of diethyl ether and dried under vacuum. Yield: 3.96 g (73%). The ethyl and isopropyl derivatives, i.e. $Et_2impy(I)_2$ and $Pr_2impy(I)_2$, were prepared under identical conditions.

Spectra data of $Me_2impy(I)_2$: ^{1}H NMR (400 MHz, d_6-DMSO, 298K): δ 9.95 (s, 1H), 9.73 (s, 1H), 9.18 (d, *J* = 6 Hz, 1H), 8.97 (d, *J* = 8 Hz, 1H), 8.46 (dd, *J* = 6, 8 Hz, 1H), 8.36 (s, 1H), 8.06 (s, 1H), 4.45 (s, 3H), 4.03 (s, 3H).

Spectra data of $Et_2impy(I)_2$: ^{1}H NMR (400 MHz, d_6-DMSO, 298K): δ 10.01 (s, 1H), 9.79 (s, 1H), 9.30 (d, *J* = 6 Hz, 1H), 9.01 (d, *J* = 8 Hz, 1H), 8.49 (dd, *J* = 6, 8 Hz, 1H), 8.41 (s, 1H), 8.17 (s, 1H), 4.74 (q, *J* = 7.2 Hz, 2H), 4.03 (q, *J* = 7.2 Hz, 2H), 1.64 (t, *J* = 7.2 Hz, 3H), 1.54 (t, *J* = 7.2 Hz, 3H).

Spectra data of $Pr_2impy(I)_2$: ^{1}H NMR (400 MHz, d_6-DMSO, 298K): δ 10.05 (s, 1H), 9.75 (s, 1H), 9.39 (d, *J* = 6 Hz, 1H), 9.03 (d, *J* = 8 Hz, 1H), 8.51 (dd, *J* = 6, 8 Hz, 1H), 8.47 (s, 1H), 8.29 (s, 1H), 5.15 (septet, *J* = 6.7 Hz, 1H), 4.80 (septet, *J* = 6.7 Hz, 1H), 1.71 (d, *J* = 6.7 Hz, 6H), 1.60 (d, *J* = 6.7 Hz, 6H).

Synthesis of $Me_2impy(PF_6)_2$. A solution of NH_4PF_6 (1.86 g, 12.1 mmol) and $Me_2impy(I)_2$ (1.64 g, 3.82 mmol) in methanol (30 mL) was stirred at RT for 2 h. The PF_6 salt was gradually precipitated out of the solution during reaction. It was collected, washed with cold methanol and diethyl ether in sequence, and dried under vacuum. Yield: 1.33 g (75%).

Spectra data of $Me_2impy(PF_6)_2$: ^{1}H NMR (400 MHz, d_6-DMSO, 298 K): δ 9.92 (s,

1H), 9.70 (s, 1H), 9.18 (d, *J* = 6 Hz, 1H), 8.97 (d, *J* = 8 Hz, 1H), 8.45 (dd, *J* = 6, 8 Hz, 1H), 8.33 (s, 1H), 8.05 (s, 1H), 4.45 (s, 3H), 4.02 (s, 3H). ^{19}F NMR (376 MHz, d_6-DMSO, 298 K): δ −70.2 (d, J_{PF} = 711 Hz). ESI-MS: m/z 174.1 $[M - 2(PF_6) - H]^+$.

Spectra data of $Et_2impy(PF_6)_2$: ^{1}H NMR (400 MHz, d_6-DMSO, 298 K): δ 9.94 (s, 1H), 9.71 (s, 1H), 9.28 (d, *J* = 6 Hz, 1H), 8.98 (d, *J* = 8 Hz, 1H), 8.47 (dd, *J* = 6, 8 Hz, 1H), 8.36 (s, 1H), 8.15 (s, 1H), 4.74 (q, *J* = 7.2 Hz, 2H), 4.03 (q, *J* = 7.2 Hz, 2H), 1.64 (t, *J* = 7.2 Hz, 3H), 1.54 (t, *J* = 7.2 Hz, 3H). ^{19}F NMR (376 MHz, d_6-DMSO, 298 K): δ −70.2 (d, J_{PF} = 711 Hz). ESI-MS: m/z 202 $[M - 2(PF_6) - H]^+$.

Spectra data of $Pr_2impy(PF_6)_2$: ^{1}H NMR (400 MHz, d_6-DMSO, 298K): δ 9.97 (s, 1H), 9.66 (s, 1H), 9.36 (d, *J* = 6 Hz, 1H), 9.00 (d, *J* = 8 Hz, 1H), 8.50 (dd, *J* = 6, 8 Hz, 1H), 8.43 (s, 1H), 8.27 (s, 1H), 5.11 (septet, *J* = 6.7 Hz, 1H), 4.80 (septet, *J* = 6.7 Hz, 1H), 1.70 (d, *J* = 6.7 Hz, 6H), 1.59 (d, *J* = 6.7 Hz, 6H). ^{19}F NMR (376 MHz, d_6-DMSO, 298 K): δ −70.2 (d, J_{PF} = 711 Hz). ESI-MS: m/z 230 $[M - 2(PF_6) - H]^+$.

Data for Single Crystal X-Ray Diffraction Studies. Single crystal X-ray diffraction data were measured on a Bruker SMART Apex CCD diffractometer using Mo radiation (λ = 0.71073 Å). The structural analysis and molecular graphics were obtained using the *SHELXTL* program. CCDC-1519153, 1519154 and 1519155 contain the supplementary crystallographic data of Pt(II) complexes **1**, **2** and **5**, respectively. These data can be obtained free of charge from the Cambridge Crystallographic Data Centre via http://www.ccdc.cam.ac.uk.

Selected crystal data of **1**: $C_{46}H_{50}F_{12}N_{14}O_3Pt_2$; M = 1465.18; T = 200(2) K; λ(Mo-K_α) = 0.71073 Å; triclinic; space group = *P*−1; *a* = 12.2448(6), *b* = 15.2481(8), *c* = 16.3269(8) Å, α = 72.0438(10), β = 69.3280(10), γ = 68.7506(9)°; *V* = 2600.7(2) Å^3; *Z* = 2; ρ_{calcd} = 1.871 Mg·cm^{-3}; μ = 5.472 mm^{-1}; *F*(000) = 1424; crystal size = 0.30 × 0.21 × 0.13 mm^3; 33638 reflections collected, 11905 independent reflections (R_{int} = 0.0399), max. and min. transmission = 0.5365 and 0.2906, restraints / parameters = 37 / 714, GOF = 1.043, final $R_1[I > 2\sigma(I)]$ = 0.0344 and wR_2(all data) = 0.0817, largest diff. peak and hole = 1.820 and −0.852 e·Å^{-3}.

Selected crystal data of **2**: $C_{18}H_{13}F_6N_7Pt$; M = 636.44; T = 200(2) K; λ(Mo-K_α) = 0.71073 Å; monoclinic; space group = $P2_1/n$; a = 13.0433(8), b = 7.4359(4), c = 19.8943(12) Å, β = 96.6100(10)°; V = 1916.70(19) Å^3; Z = 4; ρ_{calcd} = 2.206 Mg·cm^{-3}; μ = 7.401 mm^{-1}; F(000) = 1208; crystal size = 0.20 × 0.20 × 0.15 mm^3; 14296 reflections collected, 4416 independent reflections (R_{int} = 0.0381), max. and min. transmission = 0.4032 and 0.3192, restraints / parameters = 44 / 319, GOF = 1.066, final $R_1[I > 2\sigma(I)]$ = 0.0334 and wR_2(all data) = 0.0805, largest diff. peak and hole = 2.141 and −0.599 e·Å^{-3}.

Selected crystal data of **5**: $C_{19}H_{15}F_6N_7Pt$; M = 650.47; T = 200(2) K; λ(Mo-K_α) = 0.71073 Å; orthorhombic; space group = Pnma; a = 21.8036(14), b = 6.7963(4), c = 13.7863(9) Å; V = 2042.9(2) Å^3; Z = 4; ρ_{calcd} = 2.115 Mg·cm^{-3}; μ = 6.946 mm^{-1}; F(000) = 1240; crystal size = 0.45 × 0.10 × 0.10 mm^3; 15329 reflections collected, 2539 independent reflections (R_{int} = 0.0423), max. and min. transmission = 0.5434 and 0.1461, restraints / parameters = 22 / 206, GOF = 1.130, final $R_1[I > 2\sigma(I)]$ = 0.0239 and wR_2(all data) = 0.0575, largest diff. peak and hole = 0.918 and −0.674 e·Å^{-3}.

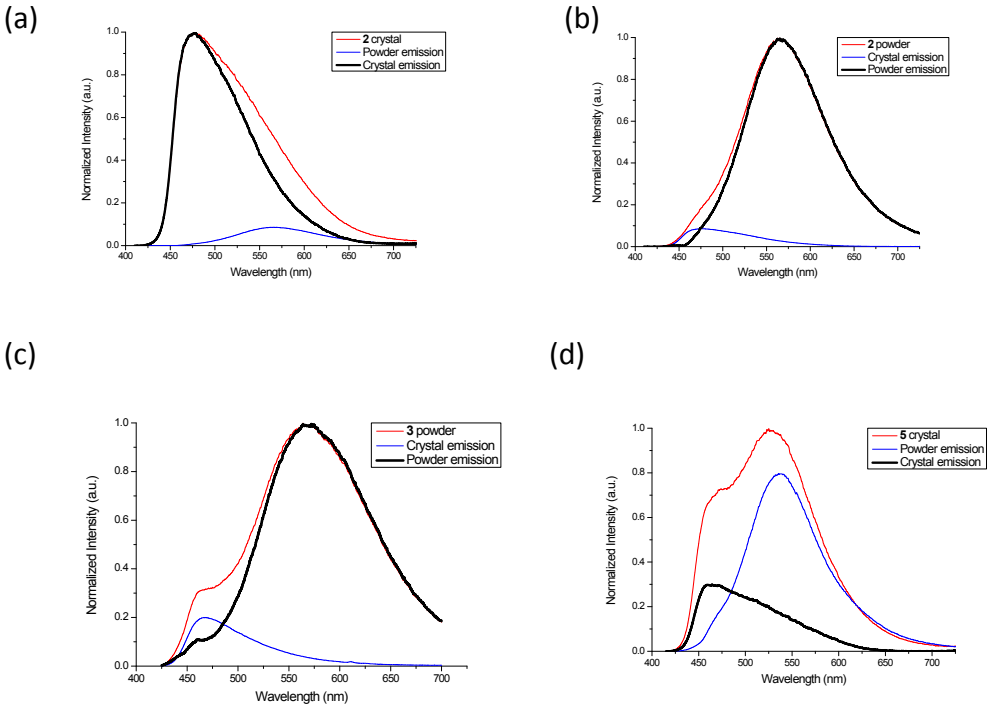

Figure S1. Band fitting in emission spectra where both high and low energy emissions are present in mixed crystalline and powdered forms; (a) **2**-crystal, (b) **2**-powder, (c) **3**-powder and (d) **5**-crystal.

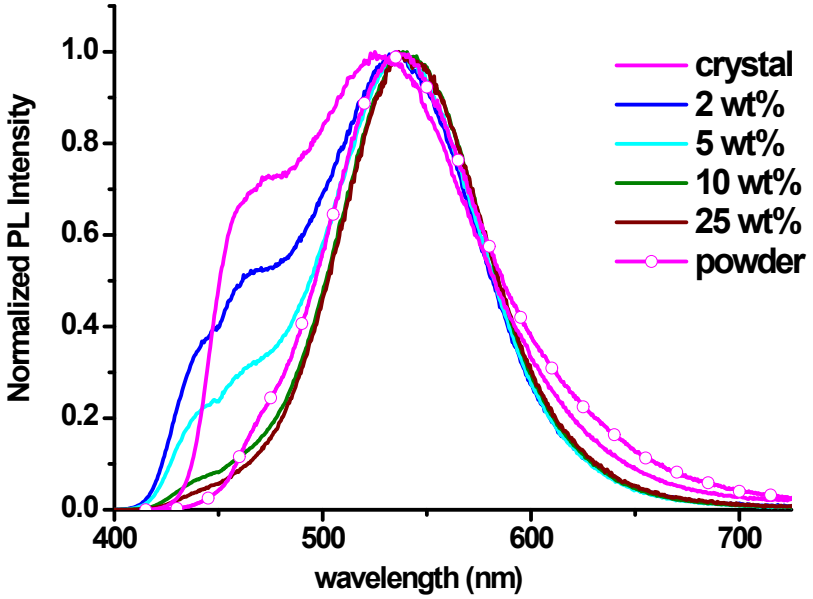

Figure S2. Photoluminescence spectra of the PMMA films with concentrations of Pt(II) complex **5** varied between 2 wt.% and 25 wt.%, together with that of polycrystalline sample (solid line) and powder (with circle) as reference.

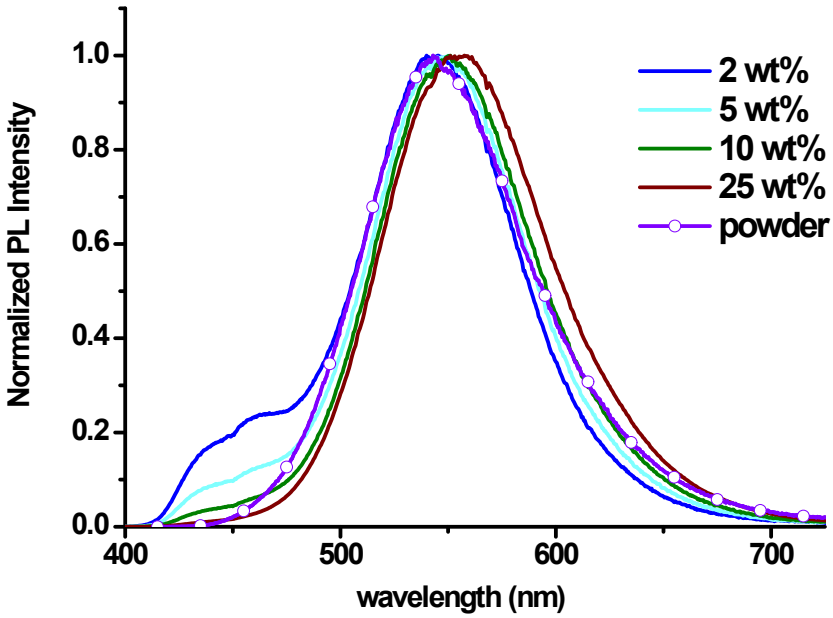

Figure S3. Photoluminescence spectra of the PMMA films with Pt(II) complex **7** varied between 2 wt.% and 25 wt.%, together with that of powder (with circle) as reference.

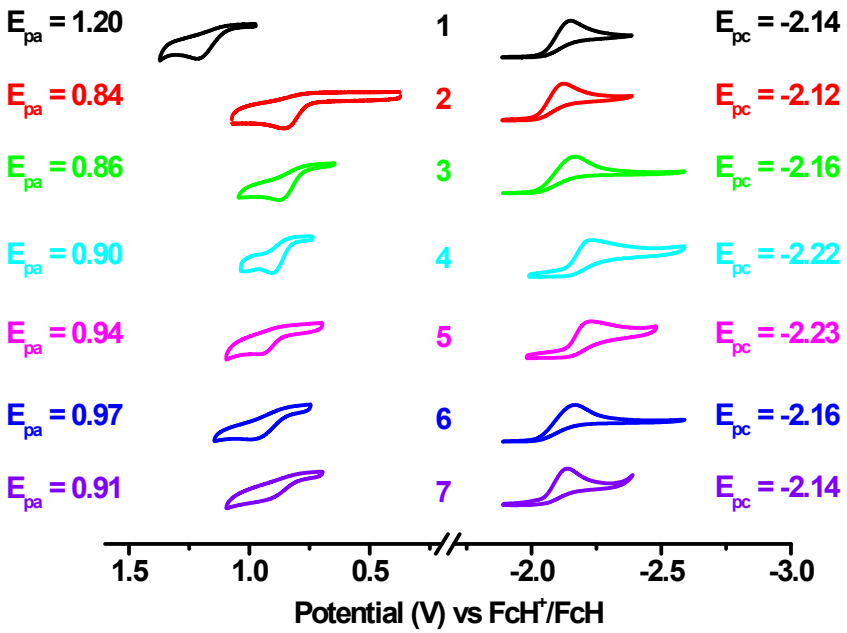

Figure S4. Cyclic voltammograms of the studied Pt(II) complexes **1** – **7**.

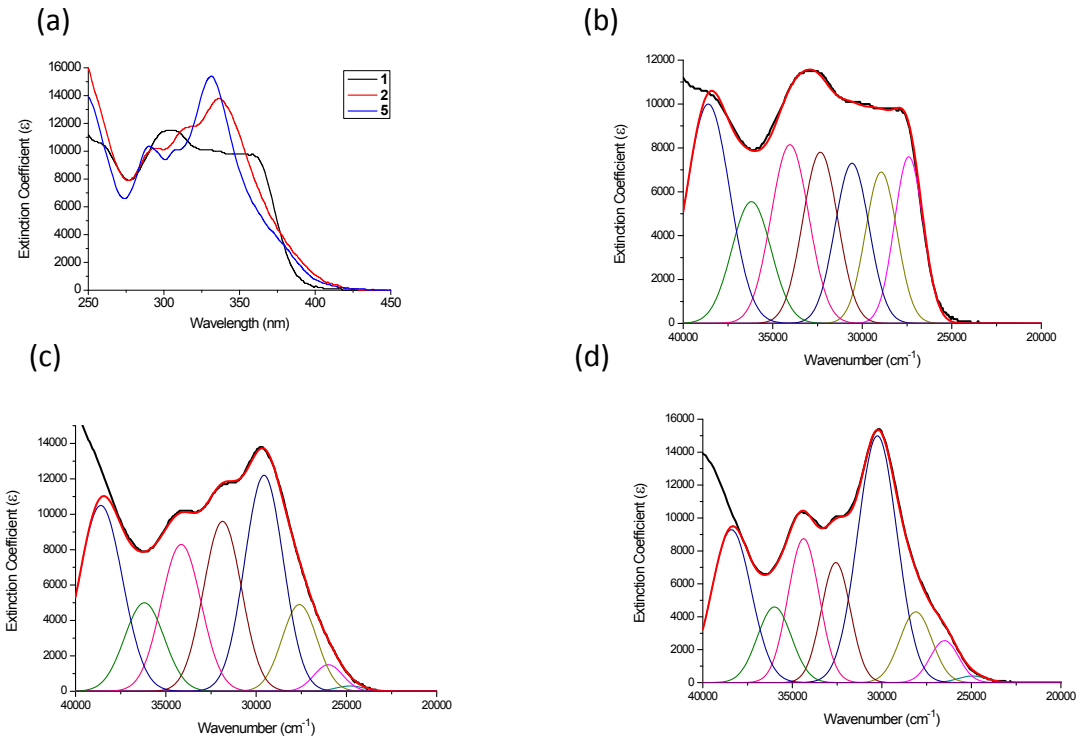

Figure S5. (a) Observed absorption spectra for **1** , **2** and **5**. Spectra with Gaussian deconvolution analyses (b) for **1**, (c) for **2** and (d) for **5**.

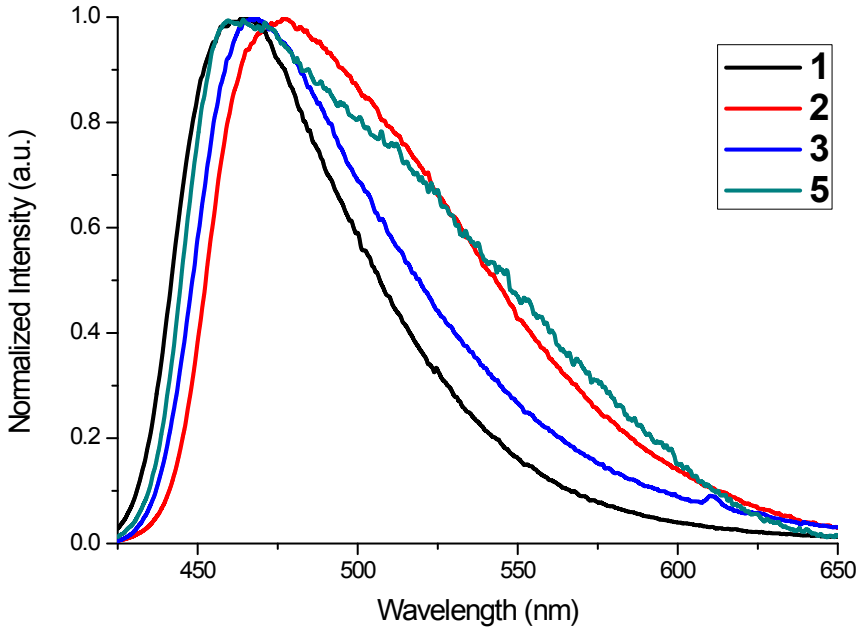

Figure S6. Observed solid state emissions from crystalline forms only.

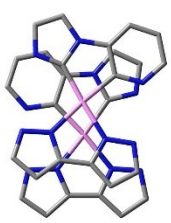

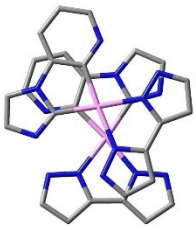

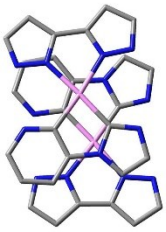

	$[\mathbf{8}]_2$ D	$[\mathbf{8}]_2$ E	$[\mathbf{8}]_2$ F
Relative Energy (kcal mol^{-1})	11.2	9.8	2.1
Pt…Pt (Å)	3.783	3.596	3.848

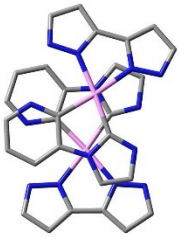

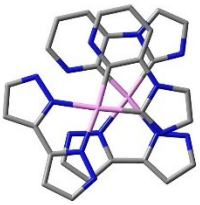

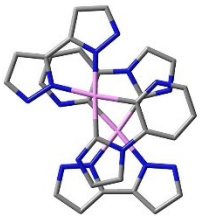

	$[\mathbf{8}]_2$ G	$[\mathbf{8}]_2$ H	$[\mathbf{8}]_2$ I
Relative Energy (kcal mol^{-1})	1.4	8.2	7.7
Pt…Pt (Å)	3.982	3.801	3.883

Figure S7. Optimized ground state (S_0) geometries of $[\mathbf{8}]_2$, D – I.

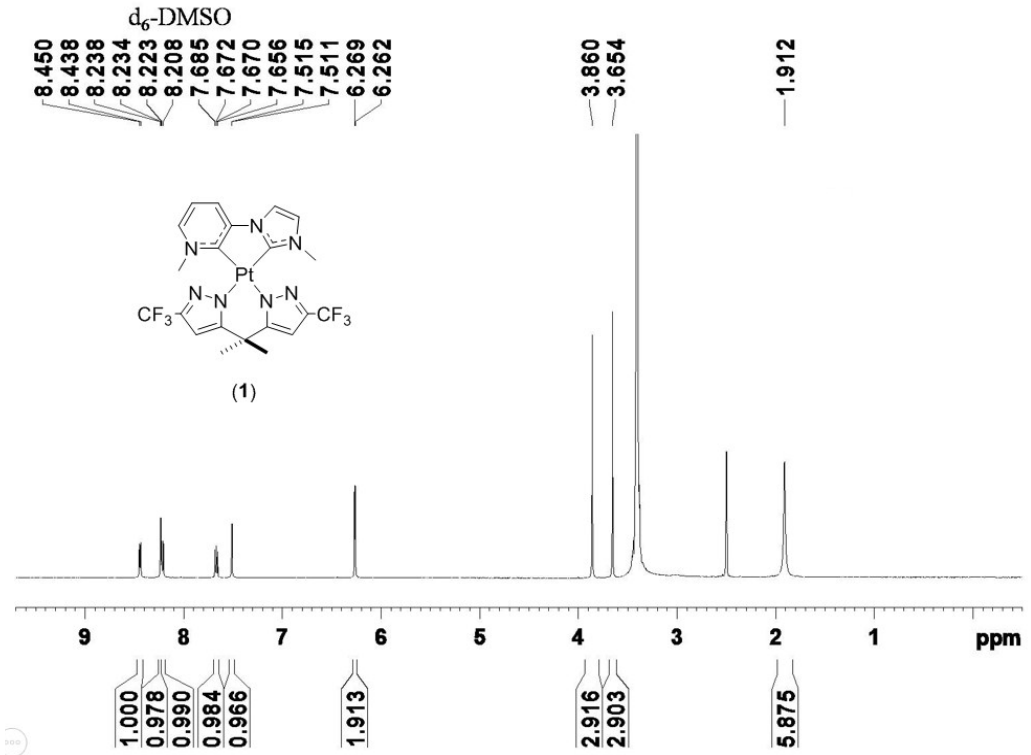

Figure S8. ^{1}H NMR spectra of **1** in d_6-DMSO solution.

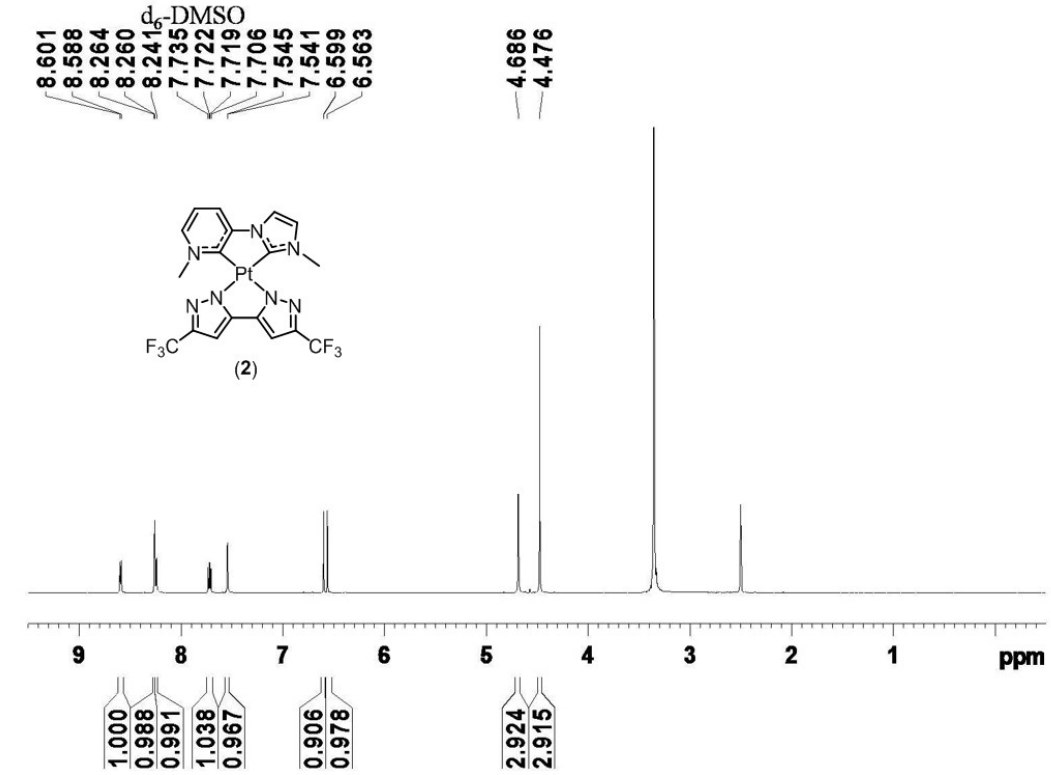

Figure S9. ^{1}H NMR spectra of **2** in d_6-DMSO solution.

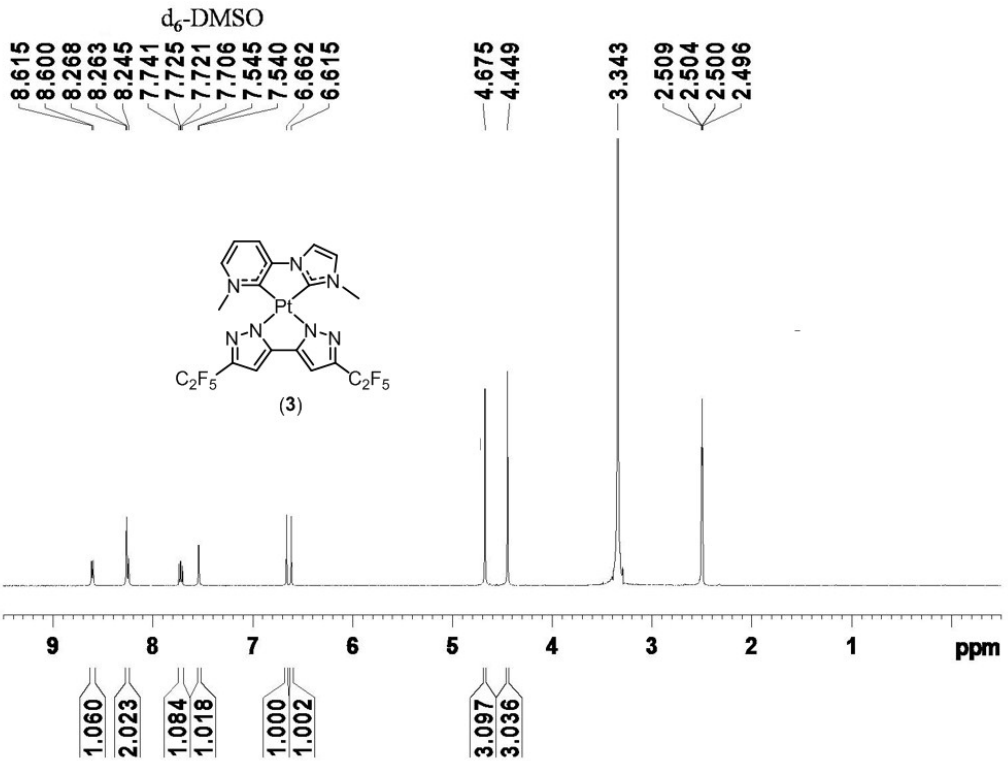

Figure S10. ^{1}H NMR spectra of **3** in d_6-DMSO solution.

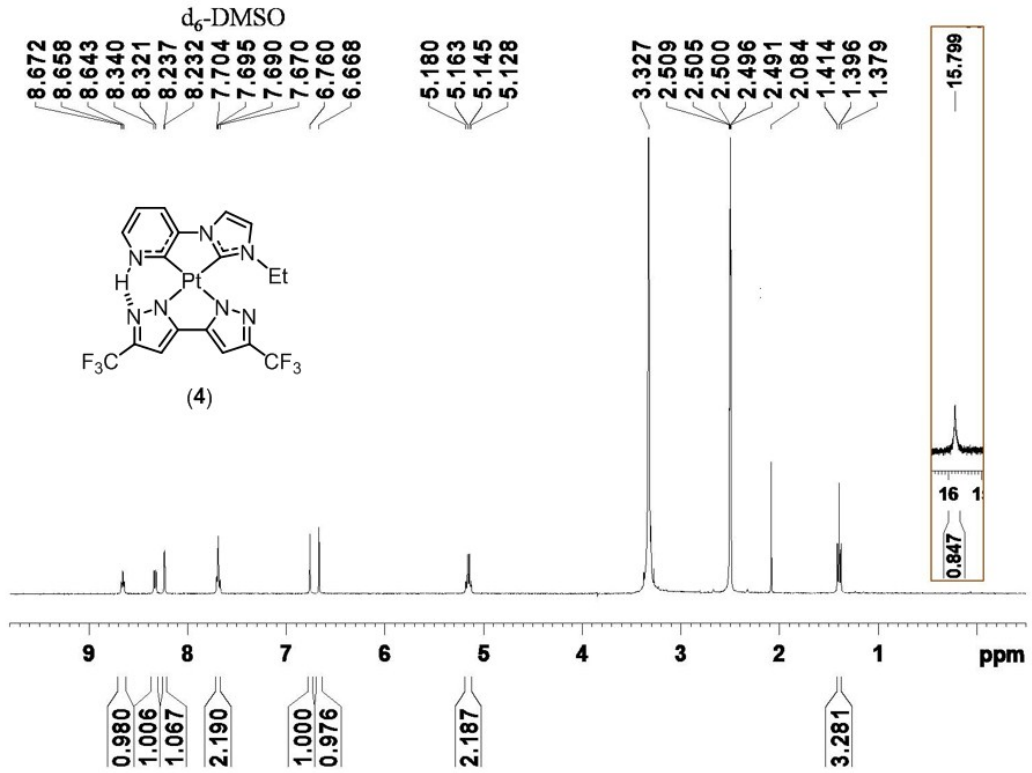

Figure S11. ^{1}H NMR spectra of **4** in d_6-DMSO solution.

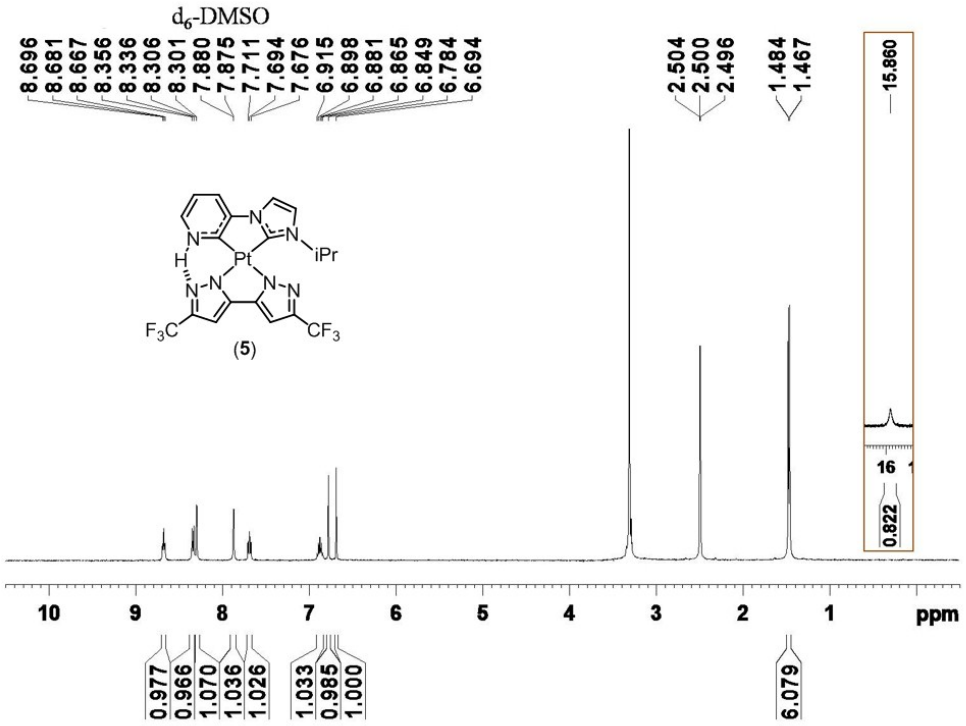

Figure S12. ^{1}H NMR spectra of **5** in d_6-DMSO solution.

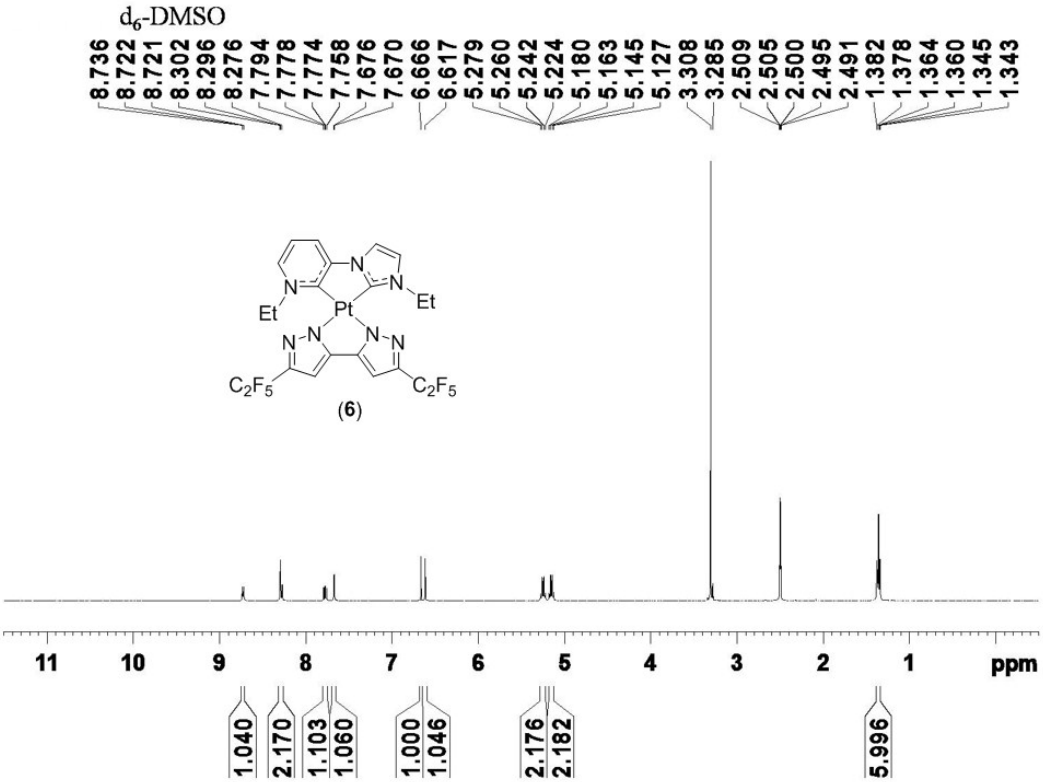

Figure S13. ^{1}H NMR spectra of **6** in d_6-DMSO solution.

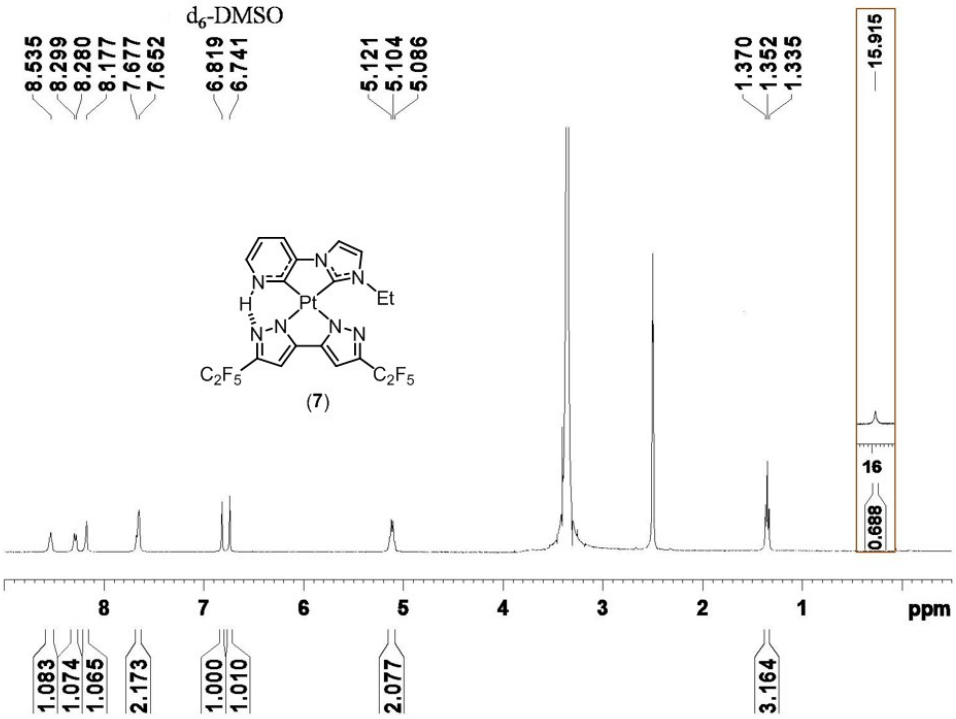

Figure S14. ^{1}H NMR spectra of **7** in d_6-DMSO solution.

Table S1. Comparison of selected geometric parameters from optimized and experimental geometries. The C-C···N-C torsion angle is a measure of the molecule planarity where C-N is the bond between the pyridine (py) and imidazole (im) rings and C-C is the bond between the two pyrazole (pz) rings.

		Pt-C(py)	Pt-C(im)	Pt-N(pzpy)	Pt-N(pzim)	C-N..C-C torsion angle
1	calculated	2.028	1.997	2.091	2.090	2.7
	X-ray	1.984(5)	1.983(4)	2.050(4)	2.054(4)	7.4
2	calculated	2.023	2.012	2.112	2.122	25.0
	X-ray	1.992(6)	1.994(6)	2.063(5)	2.058(5)	2.3
	calculated middle molecule of trimer	2.059	2.003	2.171	2.128	2.8
3	calculated	1.984	2.018	2.069	2.137	0.7
	X-ray	1.948(5)	1.994(5)	2.037(4)	2.079(5)	0.0
	calculated middle molecule of trimer	1.988	2.020	2.076	2.129	0.7

pzpy is the pyrazine ring next to the pyridine ring.

pzim is the pyrazine ring next to the imidazole ring.

Table S2. Selected orbital energies and % MO contributions of Pt, py, im and mepz/bipz units in optimized ground state monomer geometries of **1**, **2** and **5**.

1	MO	eV	Pt	py	im	mepz
	LUMO+2	-0.31	24	37	31	8
	LUMO+1	-1.74	13	57	25	5
	LUMO	-2.19	4	90	5	1
	HOMO	-6.20	20	5	9	66
	HOMO-1	-6.35	11	2	9	79
	HOMO-2	-6.41	24	7	5	65
2	MO	eV	Pt	py	im	bipz
	LUMO+2	-0.49	21	36	12	32
	LUMO+1	-1.85	12	53	27	7
	LUMO	-2.25	5	88	4	2
	HOMO	-5.79	4	1	1	94
	HOMO-1	-6.34	33	3	22	43
	HOMO-2	-6.49	31	11	3	54
5	MO	eV	Pt	py	im	bipz
	LUMO+2	-0.48	8	35	7	51
	LUMO+1	-1.85	15	48	26	10
	LUMO	-2.16	3	90	5	2
	HOMO	-5.88	7	1	2	90
	HOMO-1	-6.40	29	8	21	41
	HOMO-2	-6.56	29	9	9	53

Table S3. Selected orbital energies and % MO contributions of Pt, py, im and bipz units in optimized excited triplet state dimer geometries of $[\mathbf{8}]_2$ B and C.

B	MO	eV	Pt1	py1	im1	bipz1	Pt2	py2	im2	bipz2
	LUMO+2	-1.61	7	30	21	5	4	18	13	2
	LUMO+1	-1.84	1	54	4	0	1	34	4	0
	LUMO	-2.08	4	33	1	4	3	51	3	1
	HOMO	-4.88	3	1	1	94	0	1	0	0
	HOMO-1	-5.41	0	1	0	0	5	1	1	91
	HOMO-2	-5.96	1	1	0	2	22	7	8	59
C	MO	eV	Pt1	py1	im1	bipz1	Pt2	py2	im2	bipz2
	LUMO+2	-1.71	7	25	13	5	7	25	13	5
	LUMO+1	-1.93	1	45	3	1	1	45	3	1
	LUMO	-2.09	3	43	2	2	3	43	2	2
	HOMO	-5.07	39	2	2	7	39	2	2	7
	HOMO-1	-5.31	4	1	1	47	4	1	1	42
	HOMO-2	-5.32	3	0	1	43	3	0	1	48